


# Activation of canonical inflammasome complex by acute silica exposure in experimental rat model

Yingmei Niu <sup>1,\*</sup>, Shuangli Yang<sup>1</sup>, Xiumei Hu<sup>2</sup>

<sup>1</sup>Occupational Disease and Toxicology Department, Beijing Chao-Yang Hospital, Capital Medical University, Beijing 100020, China,

<sup>2</sup>Department of Pathology, Beijing Chao-Yang Hospital, Capital Medical University, Beijing 100020, China

\*Correspondence address. Occupational Disease and Toxicology Department, Beijing Chao-Yang Hospital, Capital Medical University, Beijing 100020, China. E-mail: inmay79@sina.com

Silicosis is a chronic irreversible pulmonary disease caused by the inhalation of silica crystals in occupational settings in most cases. Persistent inflammation in the alveolar space is considered to be the major reason for tissue damage and lung fibrogenesis. The mechanisms by which silica exposure activates immune cells are not well understood. Here, we employed an *in vivo* silicosis disease model by intratracheal instillation of a large dose of silica suspension in rats and explored the involvement of inflammasome activation. Marked leukocyte infiltration and edema were observed 3 days following silica exposure in treated animals compared to controls. Using this model, we compared the expression of inflammasome sensors (AIM2 and NLRP3) and effector protein (caspase-1) by western blot and immunohistochemical staining using the lung homogenates and lung tissue sections. Our results demonstrated that following acute silica exposure, AIM2, NLRP3 and caspase-1 expressions were increased in macrophages or/and lung epithelial cells compared to control animals. We also analyzed interleukin 1 $\beta$  expression using lung homogenates, and significant increase in interleukin 1 $\beta$  was observed in 3-day silica-exposed rats. The activation of inflammasome sensors AIM2 and NLRP3 suggested to us that blocking these activators may attenuate silica-associated tissue damage and inflammation.

**Key words:** inflammasome; silica; silicosis; occupational disease; pyroptosis.

## Introduction

Silicosis is a chronic interstitial pulmonary disease that is often related to occupational exposure to dust particles containing free crystalline, also known as silica [1]. The industrial settings that cause silicosis include, but not limited to, mining, steel industry, construction, plaster or drywall installation, glass manufacturing, and road repair [2]. It is estimated that there are >3 million workers in the USA exposed to silica dust, and it is reported that in China ~20 000 new patients are diagnosed with silicosis annually [3]. The symptoms of silicosis include shortness of breath, fatigue, chest pain, and flu-like severe cough and fever, but the diagnosis is usually made 10–35 years after initial exposure, which leads to poor recovery [4]. Silicosis patients are vulnerable to other lung complications, such as tuberculosis, chronic obstructive pulmonary disease, and lung cancer [5, 6]. Therefore, silicosis is a deliberating occupational disease worldwide, which needs better treatments urgently.

The pathogenesis of silicosis has been widely studied and a persistent inflammatory response and fibrogenesis caused by particle-induced cell injury and immune defense are regarded as the main driving factors of silicosis [7]. However, the crucial cellular and molecular mechanisms that mediate these outcomes remain

by and large unknown. Inflammasome is a multi-protein complex that is involved in innate immune response against microbial pathogens invasion and cell damage [8]. Activation of inflammasome complex causes autocatalytic cleavage and maturation of caspase-1, which further leads to the processing of precursors of interleukin 1 $\beta$  (IL-1 $\beta$ ) and IL-18 into their mature and bioactive forms [9]. The activation of these proinflammatory cytokines enables a rapid cascade of inflammatory reactions, leading to pyroptosis and death of tissue [10]. Structurally, a canonical inflammasome complex comprises three major components, namely, the upstream sensor protein such as pattern recognition receptors (PRRs), the adaptor protein called apoptosis-associated speck-like protein containing a caspase recruitment domain (CARD) (ASC), and the effector protein, pro-caspase-1 [11]. There are two families of initial PRRs, the nucleotide oligomerization domain (NOD)-like receptor (NLR) family and the pyrin and hematopoietic interferon-inducible nuclear antigens domain-containing protein (PYHIN) family [12, 13]. NLR family pyrin domain (PYD) containing 3 (NLRP3) and absent in melanoma 2 (AIM2) are among the key signal sensor components of inflammasome [14–16]. Upon ligand binding, the sensor proteins underwent conformational change and oligomerization, initiated inflammasome assembly, and

led to a variety of inflammatory processes [17]. Caspase-1 is the effector component of inflammasome and belongs to the cysteine-aspartic acid protease (caspase) family. Its activation needs proteolytic processing at conserved aspartic residues to produce two subunits, large and small, that dimerize to form the active enzyme. Activated caspase-1 proteolytically cleaves the precursor of IL-1 $\beta$  and IL-18 to produce mature cytokines, which are involved in the processes such as inflammation, septic shock, and wound healing [18]. Given the inflammatory and fibrogenic pathological features of the lung tissues damaged by silicosis, we hypothesize that activation of inflammasome may be one of the underlying molecular bases of silicosis.

Animal model is a useful tool to investigate disease pathogenesis and treatment response, whereas human silicosis is a long latency disease, difficult to mimic experimentally. Therefore, acute silicosis, which develops after intensive inhalation exposure over several days, is well reproduced in laboratory animal models [19]. Intratracheal (IT) instillation of large doses of silica suspension is a simple acute silicosis disease model in which the inhaled silica particles penetrate into the alveoli and are engulfed by macrophages and neutrophils, causing diffusive fibrosis and small round scarring lumps in the lung tissue [20–22]. A single high dose of silica (~250 mg/kg body weight) was used in the current studies based on prior publications which showed induction of obvious inflammation and lung damage by IT of silica at similar dose in rats [23]. Using this authentic model, we investigated the activation of the inflammasome during acute silica exposure.

## Methods and Materials

### Animals

Eight-week-old male Wistar rats ( $n = 24$ ) weighing 200–220 g were purchased from Beijing Weitong Lihua Experimental Animal Technology Co, Ltd and were maintained in a pathogen-free environment. The animals were kept on a 12-h light–dark cycle with free access to food and water. The animal experimental protocol (factors involved in SO<sub>2</sub> induced pulmonary fibrosis, 2020-animal-275) was approved by the Animal Ethical Committee of Capital Medical University.

### Preparation of silica suspension and IT instillation

Crystalline silica powder with a mean size of 0.8  $\mu\text{m}$  was purchased from Sigma-Aldrich. The silica was autoclaved immediately before use and then was suspended in sterile pharmacological grade saline at a concentration of 50 mg/ml. The silica suspension was sonicated and vigorously vortexed before administration. The rats were anesthetized using an i.p. injection of sodium pentobarbital (5 mg/100 g body weight). For the treatment group ( $n = 16$ ), the animals received a single trans-oral IT of silica suspension of 1 ml as described previously

[23]. The control group animals ( $n = 8$ ) received IT of 1 ml sterile saline. Animals were sacrificed using sodium pentobarbital (120 mg/rat) on Day 1 ( $n = 8$ ) or Day 3 ( $n = 8$ ) after silica instillation. The control group animals were sacrificed 1 day after saline instillation.

### Histological examination of lung tissue

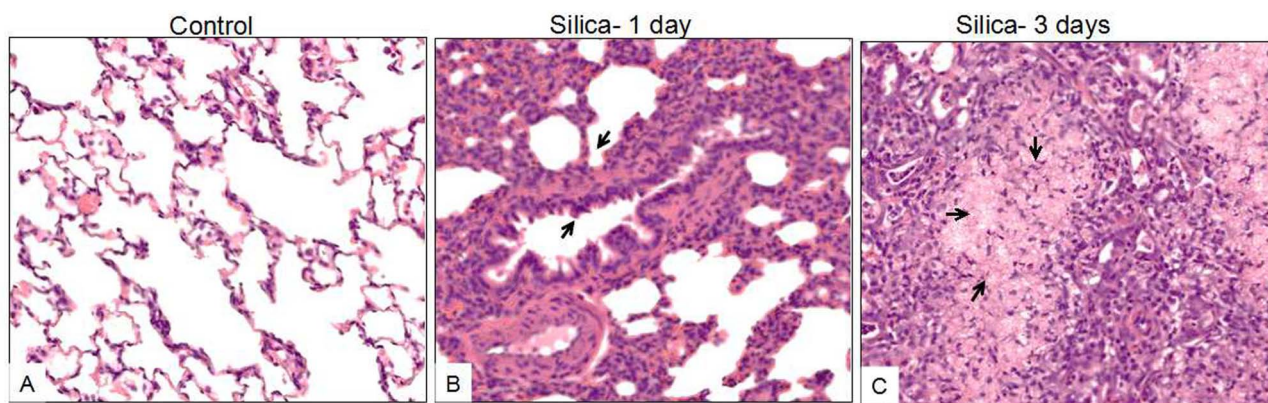
Upon experiment complement, the intact lung lobes were resected. The left lobe tissues ( $n = 5$ /group) were fixed in 10% neutral-buffered formalin and were embedded in paraffin. Serial longitudinal sections of 3  $\mu\text{m}$  thickness were cut using microtome and used for hematoxylin and eosin (H&E) staining and immunohistochemical (IHC) examination. Two pathologists independently evaluated lung tissue H&E staining and provided histopathology scores according to the degree of inflammation [24]. If there was no inflammatory cell infiltration, the tissue was scored as 0. If infiltration of inflammatory cells was observed sporadically, the tissue was scored as 1. If the infiltrating inflammatory cells formed an obvious thin layer (1–5 cell thickness) around bronchus or small blood vessels, it was scored as 2. Otherwise if a thick multi-cell layer (>five cells) of inflammatory cells was observed, it was evaluated as score 3. A total of 15 visual fields were randomly selected, and the averaged value of inflammation scores was taken as the total lung pathological inflammation score.

### IHC assessment of inflammasome components

The fixed and embedded lung sections, 3- $\mu\text{m}$  thick, were deparaffinized. Epitope retrieval was performed in citric acid-sodium citrate buffer (1 M, pH 6.0) using a pressure cooker for 15 min at 90°C. After the slides were cooling down and washed in phosphate buffered saline (PBS) for three times, they were treated in hydrogen peroxide (3%) for 10 min to inactivate endogenous peroxidase antigens. Then, the slides were blocked in 2.5% goat serum (diluted in PBS, Sigma, Cat# G9023-5ML) and were incubated with antibodies against caspase-1 (Abcam, Cat# ab1872, immunogen within the p20 subunit, 1:50), NLRP3 (Absin, Cat# abs136950, 1:100), and AIM2 (Absin, Cat# abs125828, 1:1000) for 1 h at 37°C. PBS was used in the negative control group instead of primary antibody. The slides were washed with PBS and were then incubated with peroxidase-conjugated anti-rabbit IgG (DAKO, Cat# K4003) and anti-mouse IgG (DAKO, Cat# K4001) for 0.5 h at 37°C. Staining was then performed using a 3,3'-diaminobenzidine staining kit (Thermo Fisher, Cat# TL-125-QHD). A positive reaction was indicated by brown staining in the nuclei and cytoplasm. The IHC staining was evaluated under a Zeiss Axio. Scope A1 light microscope.

### Western blot analysis

The right lobes of the resected lung tissues ( $n = 5$ /group) were cut into small pieces and lysed on ice using Dounce tissue homogenizer (Tissueprep, China) in



D Inflammation Scores of the Lung Sections Evaluated by Pathologists

Groups	Scores
Control	0.10 ± 0.01
Silica-1 day	1.10 ± 0.02*
Silica-3 days	2.10 ± 0.02*

$p < 0.05$

**Figure 1.** Histological analysis of the lung tissues from silica-exposed rats compared with controls following intratracheal instillation (IT) for 1 day and 3 days. Rats were received IT exposure to silica (50mg/mL, 1mL) or sterile saline. One day and 3 days following exposure, the animals were sacrificed and lung tissues were processed for histochemical analysis. The control animals were sacrificed one day after saline IT exposure. A comparison of the gross architecture of the lung sections from saline-exposed rats revealed normal lung structure (A). In contrast, silica-exposed rats developed features of pulmonary inflammation and edema, characteristic of rat silicosis (B & C). (D) Inflammation score of rat lung tissue was evaluated by two pathologists in a double-blind fashion, taking no inflammation as 0 score, mild inflammation as 1, overt leukocyte infiltration as 2, and massive infiltration as 3. The images were representative pictures from 5 animals of each group. 200× original magnification. \* $p < 0.05$ .

tissue lysis buffer [8 M urea, 4% CHAPS, 40 mM Tris(base), and 1% PMSF] supplemented with a cocktail of protease inhibitors (Promega) at the ratio of 250 mg tissue/1 ml lysis buffer. The supernatant was collected after centrifuge at 14000× g for 15 min. The protein concentrations were determined using BCA kit (Thermo Scientific). Equal amounts of proteins from each sample (50 μg) were resolved by SDS-PAGE, transferred to PVDF membranes, blocked with 5% skimmed milk for 1 h at 25°C, and probed at 4°C overnight with the primary antibodies against AIM2 (Absin, Cat# abs125828, 1:300) and β-actin (Beyotime, 1:1000). Blots were subsequently probed with horseradish peroxidase-conjugated anti-rabbit IgG and anti-mouse IgG (Beyotime, China) at 1:1000. Immunoreactive bands were visualized by enhanced chemiluminescence (PPLYGEN, China). Quantitation was analyzed densitometrically using ImageQuant 5.2 software (GE Healthcare, Pittsburgh, PA).

### Measurement of IL-1β in lung homogenates by enzyme-linked immunosorbent assay

The small pieces of right lobes of lung tissues ( $n = 3$ /group) were homogenized using Dounce tissue homogenizer (Tissueprep, China). The supernatant was collected after centrifuge at 14000× g for 15 min. The protein concentrations were determined using BCA kit (Thermo Scientific). The same amount of protein was used for ELSIA after protein concentration assay. IL-1β was measured using commercial enzyme-linked immunosorbent assay (ELISA) kits (Abcam, Cat# ab100767). In brief, the

same amount of lung lysis samples was applied onto a 96-well plate. Calibration curve was constructed with eight points by serially diluting a solution of recombinant rat IL-1β (10 ng/ml). The plate was incubated at room temperature for 2.5 h and washed six times with washing solution (PBS, pH 7.4 containing 0.5% of Tween). A secondary antibody was applied to each well and the plate was incubated for 20 min at 37°C. After washing, 100 μl of HRP-linked streptavidin was added to each well and the plate was placed at room temperature for 45 min. After further washing, the amount of IL-1β was determined by the addition of 3,3',5,5'-tetramethylbenzidine and was read at 450 nm after stopping the reaction by adding 2 M H<sub>2</sub>SO<sub>4</sub>.

### Statistical analysis

Student t-test was used for ELISA analysis. Statistical significance will be defined as  $P < 0.05$ . The minimum number of experimental replications was 3.

## Results

### Pulmonary pathology in rats instilled silica in comparison to control rats

Histological characteristics of silicosis [25] were observed from H&E staining of silica-exposed rat lung sections, such as inflammation and interstitial edema (Fig. 1B and C). Alveolar epithelial hyperplasia was detected following one-day silica exposure (Fig. 1B), and extensive pulmonary edema and inflammatory cell



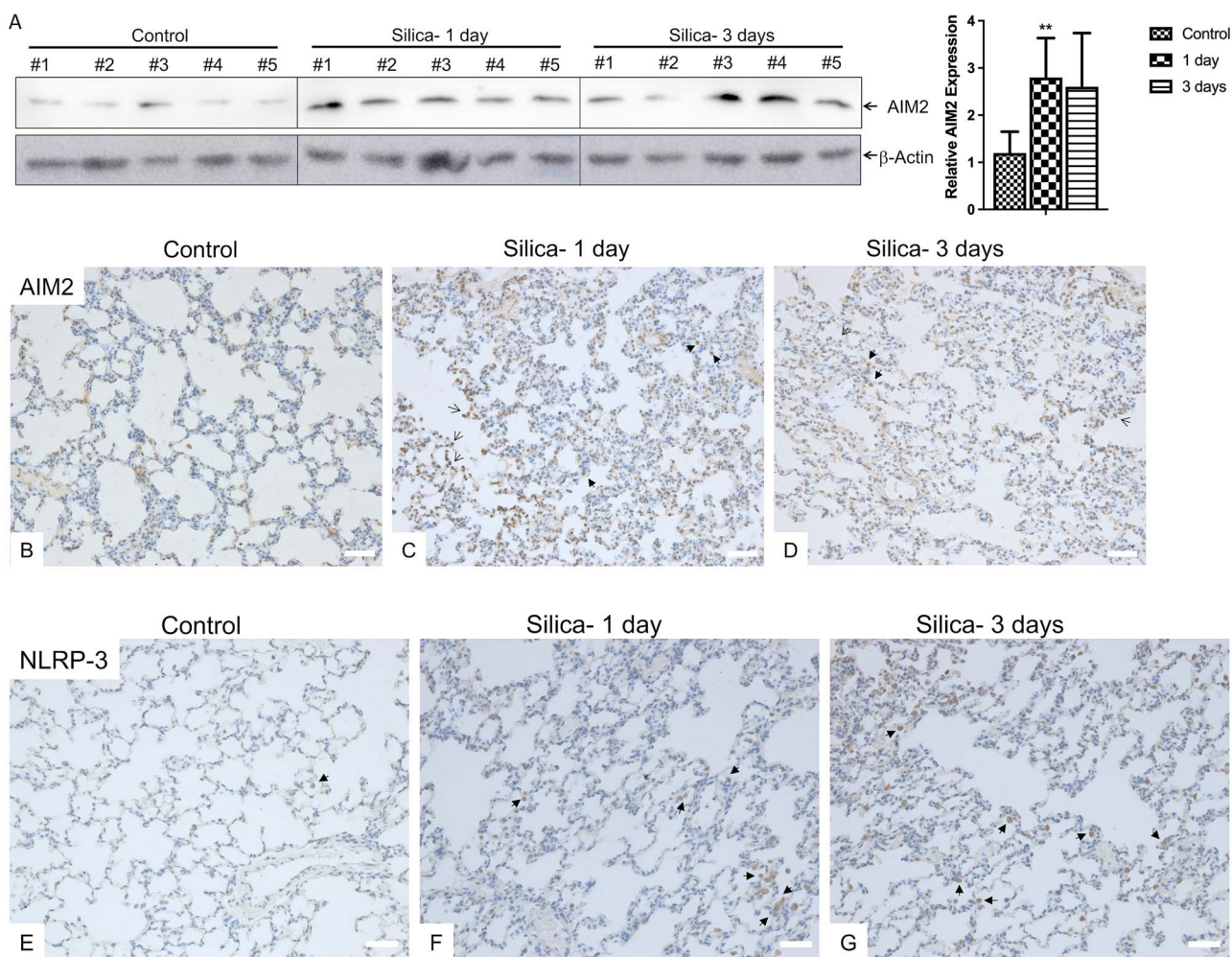


**Figure 2.** Silica exposure increased inflammasome sensor protein expression. (A) Lung tissue homogenates from the control and silica exposed rats ( $n=5$ /group) were subjected to Western Blot analysis for AIM2.  $\beta$ -Actin was used as loading control. Quantitation was analyzed densitometrically using ImageQuant 5.2 software (GE Healthcare, Pittsburgh, PA). \*\* $p < 0.01$ . (B–G) Immunochemical staining of AIM2 (B–D) and NLRP3 (E–G) was performed using the lung sections of silica exposed rats (C & F for silica 1-day, D & G for silica 3-days) and control animals (B and E). Solid arrows indicated macrophages, and open arrows indicated lung epithelial cells. Scale bars: 50  $\mu$ m.

infiltration were observed in animals after 3-day silica exposure (Fig. 1C). A comparison of the gross architecture of the lung sections from saline-exposed rats reveals the normal morphologic structure of the lung (Fig. 1A). Inflammation score of rat lung tissue was evaluated by two pathologists in a double-blind fashion, taking no inflammation as 0 score, mild inflammation as 1, overt leukocyte infiltration as 2, and massive infiltration as 3. As summarized in Fig. 1D, the scores for the lung sections of silica-exposed animals (1 day:  $1.10 \pm .02$ , 3 days:  $2.10 \pm .02$ ,  $P < 0.05$ ) were significantly higher than those in control animals ( $0.10 \pm 0.01$ ). These observations suggest acute silica exposure at high dose readily caused inflammation in animal model, which can be utilized for molecular mechanism studies.

### Inflammasome sensor proteins were increased following silica exposure

Inflammasome is a multi-protein complex that is involved in innate immune response against microbial pathogen invasion and cell damage [8]. AIM2 and NLRP3 are among the key signal sensors of inflammasome [14].

Upon ligand binding, the sensor proteins underwent conformational change and oligomerization, initiated inflammasome assembly, and led to a variety of inflammatory processes. We detected AIM2 expression in the lung homogenates of silicosis animals by western blot. As shown in Fig. 2A, AIM2 protein expression was elevated following silica-exposure for 1 day compared to control animals ( $P < 0.05$ ). In line with this, IHC staining of AIM2 demonstrated higher expression in the lung epithelial cells (nucleus, open arrows) and macrophages (cytosolic, solid arrows) of the silica-exposed animals (Fig. 2C and D) compared to control animals (Fig. 2B). Our IHC results also revealed that NLRP3 was majorly expressed in the cytosolic portion of macrophages (solid arrows, Fig. 2E), and silica exposure again increased NLRP3 expression (Fig. 2F and G).

### Changes in caspase-1 and IL-1 $\beta$ following silica exposure

Our IHC analysis revealed obviously increased cytoplasmic caspase-1 expression in the macrophages following

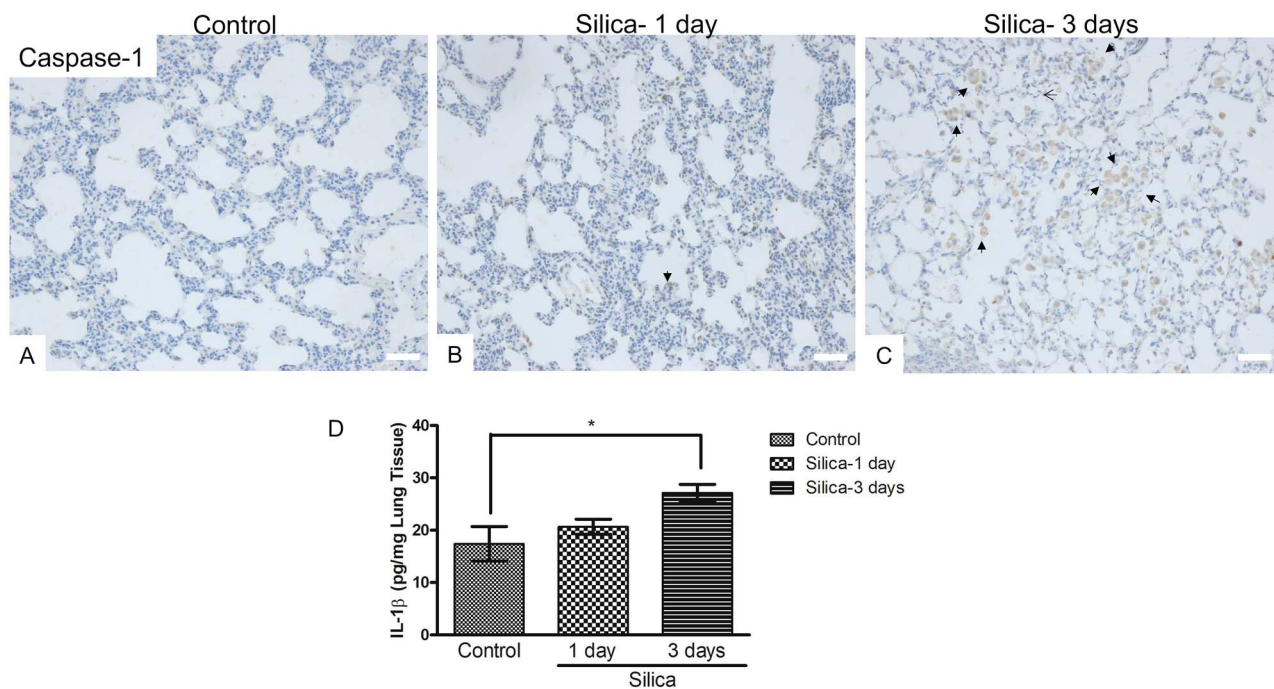


**Figure 3.** Analysis of Caspase-1 and IL-1 $\beta$  expression following silica exposure. (A–C) IHC staining of Caspase-1 was performed using the lung sections of silica exposed rats (B for silica 1-day, C for silica 3-days) and control animals (A). Solid arrows indicated macrophages, and open arrows indicated lung epithelial cells. Scale bars: 50  $\mu$ m. (D) The lung tissue homogenates from control and silica exposed rats ( $n=3$ /group) were used for ELISA analysis of IL-1 $\beta$  amount.

silica exposure for 3 days (Fig. 3C), compared to control (Fig. 3A) and the group of silica exposure for 1 day (Fig. 3B). Then, we analyzed the IL-1 $\beta$  amount using lung homogenates ( $n = 3$ /group). Our ELISA results showed a significant increase in IL-1 $\beta$  in 3-day exposed rats but not in 1-day silica-exposed animals, which may be due to short exposure period (pg/mg lung tissue, control:  $17.40 \pm 1.91$ , silica-1 day:  $20.66 \pm .84$ , silica-3 days:  $27.15 \pm .94$ , Fig. 3D), which indicated that longer silica exposure time caused activation of proinflammatory cytokine.

## Discussion

Inhalation of silica crystals into the small airways of lung not only sterically damaged the mucociliary clearance function of the lung but also raised a cascade of inflammatory response characterized by release of cytokines, such as IL-1 $\beta$  and IL-18, and factors that can induce fibrosis [10]. In our current studies, using IT silica exposure model in rats, we demonstrated activation of inflammasome sensor components (AIM2 and NLRP3) and execute protein (caspase-1) following acute silica exposure, which further led to activation of IL-1 $\beta$ . This suggested to us that blocking these activators may attenuate silica-associated tissue damage and inflammation.

The NLR family members contain modular structures, namely an N-terminal CARD or PYD, a central nucleotide-binding and oligomerization (NACHT) domain, and a C-terminal leucine-rich repeats (LRRs) [26]. The CARD and

PYD domains mediate homotypic protein–protein interactions with adaptor protein ASC for downstream signaling. The NACHT domain is conserved in all NLR family members and enables ATP-dependent oligomerization. The LRRs are believed to function in ligand sensing and autoregulation [27]. According to the sequences similarities in the NACHT domain, NLR family is further grouped into three distinct subfamilies, namely, the NODs (NOD1–2, NOD3/NLRC3, NOD4/NLRC5, NOD5/NLRX1, and CIITA), the NLRPs (NLRP1–14, also called NALPs), and the IPAF subfamily consisting of IPAF (NLRC4) and NAIP [26]. The NLRP3 inflammasome is currently the most fully characterized inflammasome. Under resting conditions, NLRP3 keeps in an autoinhibited state, and the activation signals include extracellular ATP, reactive oxygen species, K(+) efflux, crystals of monosodium urate or cholesterol, amyloid-beta fibers, environmental or industrial particles and nanoparticles, cytosolic dsRNA, etc. Using the lung tissue sections, we detected NLRP3 expression by IHC staining and demonstrated that following acute silica exposure, NLRP3 exhibited obvious increase in the macrophages compared to control animals. We observed similar changes with caspase-1, and longer exposure time (3 days) caused even higher caspase-1 changes in the macrophages.

AIM2 belongs to the PYHIN family and contains an N-terminal PYD and a conserved DNA-binding domain, named hematopoietic IFN-inducible nuclear protein with 200-amino acids (HIN-200) [14]. Cytoplasmic AIM2 maintains in an autoinhibitory state and undergoes conformational change and oligomerization after it binds cytosolic dsDNA of viral and bacterial origin,



or self-DNA from apoptotic cells in a non-sequence-specific manner. The AIM2 PYD, which is responsible for interaction with the downstream adapter protein ASC through homotypic PYD-PYD interactions, is inhibited by the HIN-200 domain in unstimulated situation. Only upon binding to the dsDNA ligand can AIM2 initiate inflammasome assembly, which indicated the highly organized order of AIM2-dependent inflammasome activation. Our IHC staining results of AIM2 revealed its expression in both epithelial cells and macrophages but with different cellular compartment locations. Silica exposure increased AIM2 expressions in both types of cells. Further studies using AIM2 knockdown (by short interfering RNA) or knockout (by CRISPR) approaches will facilitate the elucidation of role of AIM2 in silica-induced inflammasome activation.

In summary, in our current studies, we employed an *in vivo* silicosis disease model and explored the expressions of inflammasome components. Our studies have demonstrated exclusive upregulations of AIM2, NLRP3, and caspase-1 following acute silica exposure, which led to the activation of IL-1 $\beta$  3 days after exposure. The activation of inflammasome sensors suggested to us that pyroptosis is the pathway of lung damage. Further studies on the antagonists of these activators may warrant novel treatment options for silicosis patients.

## Conclusion

Using intratracheal instillation of large doses of silica suspension as a simple acute silicosis disease model, we demonstrated activation of inflammasome sensor components and execute protein following acute silica exposure, indicative of a molecular mechanism of silica-associated tissue damage and inflammation.

## Authors' contributions

Yingmei Niu conceived and designed the experiments, contributed reagents/materials/analysis tools, and wrote the paper. Yingmei Niu and Shuangli Yang performed the experiments. Yingmei Niu and Xiumei Hu analyzed the data.

## Acknowledgements

Not applicable.

## Conflict of interest statement

None declared.

## Ethics approval

All animal experiments were approved by Animal Ethical Committee of Capital Medical University (Beijing,

China, No.020-animal-275). All animal experiments were carried out in accordance with relevant guidelines and regulations. All animal experiments were carried out in compliance with the ARRIVE guidelines.

## Funding

This research received no specific grant from any funding agency.

## References

- Graham WG. Silicosis. *Clin Chest Med* 1992;**13**:253–67.
- Greenberg MI, Waksman J, Curtis J. Silicosis: a review. *Dis Mon* 2007;**53**:394–416.
- Hui Z, Dingjie X, Yuan Y et al. Silicosis decreases bone mineral density in rats. *Toxicol Appl Pharmacol* 2018;**348**:117–22.
- Pollard KM. Silica, silicosis, and autoimmunity. *Front Immunol* 2016;**7**:97.
- Nasrullah M, Mazurek JM, Wood JM et al. Silicosis mortality with respiratory tuberculosis in the United States, 1968–2006. *Am J Epidemiol* 2011;**174**:839–48.
- Barnes H, Goh NSL, Leong TL et al. Silica-associated lung disease: an old-world exposure in modern industries. *Respirology* 2019;**24**:1165–75.
- Mossman BT, Churg A. Mechanisms in the pathogenesis of asbestosis and silicosis. *Am J Respir Crit Care Med* 1998;**157**:1666–80.
- Abdul-Sater AA, Philpott DJ. Inflammasomes. In: Ratcliffe MJH (ed.), *Encyclopedia of Immunobiology*. Oxford: Academic Press, 2016, 447–53.
- Harijith A, Ebenezer DL, Natarajan V. Reactive oxygen species at the crossroads of inflammasome and inflammation. *Front Physiol* 2014;**5**:1–11.
- Hornung V, Bauernfeind F, Halle A et al. Silica crystals and aluminum salts activate the NALP3 inflammasome through phagosomal destabilization. *Nat Immunol* 2008;**9**:847–56.
- Song N, Li T. Regulation of NLRP3 inflammasome by phosphorylation. *Front Immunol* 2018;**9**:1–9.
- Fernandes-Alnemri T, Yu JW, Datta P et al. AIM2 activates the inflammasome and cell death in response to cytoplasmic DNA. *Nature* 2009;**458**:509–13.
- Broz P, Monack DM. Molecular mechanisms of inflammasome activation during microbial infections. *Immunol Rev* 2011;**243**:174–90.
- Schattgen S, Fitzgerald K. The PYHIN protein family as mediators of host defenses. *Immunol Rev* 2011;**243**:109–18.
- Peeters PM, Eurlings IMJ, Perkins TN et al. Silica-induced NLRP3 inflammasome activation *in vitro* and in rat lungs. *Part Fibre Toxicol* 2014;**11**:58–8.
- Lang T, Lee JPW, Elgass K et al. Macrophage migration inhibitory factor is required for NLRP3 inflammasome activation. *Nat Commun* 2018;**9**:2223.
- Jin T, Perry A, Smith P et al. Structure of the absent in melanoma 2 (AIM2) pyrin domain provides insights into the mechanisms of AIM2 autoinhibition and inflammasome assembly. *J Biol Chem* 2013;**288**:13225–35.

18. Boucher D, Monteleone M, Coll RC *et al.* Caspase-1 self-cleavage is an intrinsic mechanism to terminate inflammasome activity. *J Exp Med* 2018;**215**:827–40.
19. Davis GS, Leslie KO, Hemenway DR. Silicosis in mice: effects of dose, time, and genetic strain. *J Environ Pathol Toxicol Oncol* 1998;**17**:81–97.
20. Borges VM, Lopes MF, Falcão H *et al.* Apoptosis underlies immunopathogenic mechanisms in acute silicosis. *Am J Respir Cell Mol Biol* 2002;**27**:78–84.
21. Foster WM, Walters DM, Longphre M *et al.* Methodology for the measurement of mucociliary function in the mouse by scintigraphy. *J Appl Physiol* (1985) 2001;**90**:1111–7.
22. Rao GVS, Tinkle S, Weissman D *et al.* Efficacy of a technique for exposing the mouse lung to particles aspirated from the pharynx. *J Toxicol Environ Health A* 2003;**66**:1441–52.
23. Peng HB, Wang RX, Deng HJ *et al.* Protective effects of oleanolic acid on oxidative stress and the expression of cytokines and collagen by the AKT/NF- $\kappa$ B pathway in silicotic rats. *Mol Med Rep* 2017;**15**:3121–8.
24. Tournoy KG, Kips, Schou *et al.* Airway eosinophilia is not a requirement for allergen-induced airway hyperresponsiveness. *Clin Exp Allergy* 2000;**30**:79–85.
25. Beamer CA, Migliaccio CT, Jessop F *et al.* Innate immune processes are sufficient for driving silicosis in mice. *J Leukoc Biol* 2010;**88**:547–57.
26. Schroder K, Tschopp J. The inflammasomes. *Cell* 2010;**140**:821–32.
27. Lamkanfi M, Dixit VM. Mechanisms and functions of inflammasomes. *Cell* 2014;**157**:1013–22.